Chapter 3

Fundamental characteristics governing dynamics of whirlwinds: Application to dust devils

3.1 Introduction

Rotating columnar fluid masses called vortex have been extensively investigated to model their flow patterns under different considerations by simplifying the complexity inherent to the solutions. This led to several solutions, of course special ones, fit for special circumstances formulated under different boundary conditions. The struggle for a general solution is no doubt continuing unabated across the scientific world.

The contents of this chapter are published in Zeitschrift für Naturforschung A, 72(8), 763-778, (2017).

Vortex exits in nature in various forms and it is known by different names, depending on its size, strength, longivity, and the country of its occurrence. It is, of course, also dependent on the language spoken in the area. Among them tornado, typhoon, cyclone, hurricane, whirlwind etc. are common names.

A tornado is a very strongly rotating funnel shaped vortex stretching up to the sky and connected to clouds. Hurricane is a tropical cyclone occurring in the southern Atlantic ocean, Caribbean seas, Gulf of Mexico and the eastern Pacific Ocean. It does not touch clouds. It is characterised by heavy rains produced by strong winds and rapidly rotating spiral thunderstorms around a centre of low pressure. Typhoon is a mature tropical cyclone observed in the North Pacific Ocean. Whirlwind is a very tiny and transient rotating wind mixed with dust particles, dry leaves and anything available around, lying on the ground prior to its birth and light enough to float in the air, observed particularly in summer.

Among the initial attempts to model a vortex type phenomenon was an effort by Rankine (1882). He presented his tornado vortex model with the assumptions of simple steady-state rotation of a radially symmetric circular solid mass possessing only azimuthal velocity (i.e. rotational velocity about the axis of symmetry) and with the outer region being free from vorticity. That simplest model described by him with the assumptions that the radial and axial velocities are negligibly small, i.e., respectively $u = 0$, $w = 0$, is given by $v = v_0 r/a$ for $r < a$ and $v = v_0 a/r$ for $r > a$, where r, a, v and v_0 are radial coordinate, radius of the vortex, azimuthal velocity and the maximum azimuthal velocity at $r = a$. The part of the motion beyond the core vortex is called free vortex whose velocity, unlike the core vortex, in inversely proportional to the radial distance.

The velocity profile of Tayler (1918) vortex is given by $u = 0$, $w = 0$, and $v(r,t) = Mr/8\pi\nu t^2 \exp(-\frac{r^2}{4\nu t})$, where M represents the total angular momentum about the axis given by $M = \int_0^\infty 2\pi r^2 v dr$. This solution has zero total circulation

and finite angular momentum M.

An unsteady axisymmetric columnar vortex model known as Oseen-Lamb model (Oseen, 1912; Lamb, 1932) incorporated viscous and unsteady aspects of the flow and modified it to: radial velocity is negligibly small, i.e., $u = 0$, the axial velocity is negligibly small, i.e., $w = 0$ and the azimuthal velocity is given by $v(r,t) = \frac{\Gamma_0}{2\pi r}\{1 - \exp(-\frac{r^2}{4\nu t})\}$, where $\Gamma(r,t) = 2\pi r v$, $\{\Gamma(0,0) = 0, \Gamma(0,t) = 0, \Gamma(\infty,t) = \Gamma_0\}$, Γ, t and v represent circulation, time and kinematic viscosity respectively.

Burgers (1940, 1948) and Long-Rott (Long, 1957; Rott, 1958) independently obtained Burgers-Rott vortex model for steady viscous vortex embedded in a radially inward stagnation point flow over a plane boundary in the form: the radial velocity is $u = -ar$, the axial velocity is $w = 2az$, and the azimuthal velocity is given by $v(r,t) = \frac{\Gamma_0}{2\pi r}\{1 - \exp(-\frac{ar^2}{2\nu})\}$, where $a = -(\partial u/\partial r)_0$.

Sullivan (1959) vortex model is an exact solution and has some similarity to the Burgures-Rott vortex model. There is a one-celled vortex and a two-celled vortex as well. The two-celled vortex has an inner cell in which air flow descends from above and flows outward to meet a separate air flow that is converging radially. Both flows rise at the point of meeting. The Sullivan vortex is probably the simplest vortex that can describe the flow in an intense tornado with a central downdraft, and it is a simplest vortex that localizes its updraft to a particular place-there is a place for the thunderstorm. The mathematical form of the Sullivan Vortex is: $u = -ar + \frac{6\nu}{r}(1 - \exp(-\frac{ar^2}{2\nu}))$, $w = 2az(1 - 3\exp(-\frac{ar^2}{2\nu})$ and $v = \frac{\Gamma}{2\Pi r}\frac{H(\frac{ar^2}{2\nu})}{H(\infty)}$, where Γ is the circulation strenght of the vortex, $a = -(\partial u/\partial r)_0$ is the strength of the suction and $H(x)$ is the function defined as $H(x) = \int_0^x \exp(f(t))$, where $f(t) = -t + 3\int_0^t (1 - \exp(-y))dy/y$. ν is considered to be a constant eddy viscosity which dominates the value of this coefficient, not molecular viscosity. Moreover, the distribution pressure in the atmosphere is given as $p(r,z) = p_0 + \rho\int_0^r \frac{v^2}{r}dr - \frac{\rho r^2}{2}(r^2 + 4z^2) - \frac{18\rho v^2}{r^2}(1 - \exp(-\frac{ar^2}{2\nu}))$. The axial pressure gradient is $\partial p/\partial z = -4\rho z a^2$, and increase vertically without bound.

Batchelor (1964) vortex is an approximate solution to the Navier-Stokes equations obtained using a boundary layer approximation. The physical reasoning behind this approximation is the assumption that the axial gradient of the flow field of interest is of much smaller magnitude than the radial gradient. The solution presented are meant for trailing line vortices from lifting surfaces, jet intake vortices, bath drain vortices, tornadoes etc.

The most simplified form of the Batchelor vortex is $q-$vortex. It is axisymmetric stretch free columnar vortex. A $q-$vortex is a model of isolated vortex flow with both axial and azimuthal velocity components. The $q-$vortex are defined by $u = 0$, $w = \frac{\Gamma_0}{2\pi aq}\{1 - \exp(-r^2/a^2)\}$, and $v = \frac{\Gamma_0}{2\pi r}\{1 - \exp(-r^2/a^2)\}$, where a is the core radius, q is the swirling parameter, the initial parameter Γ_0 is an arbitary parameter.

The Vatistas (1991), proposed the tangential velocity profiles for vortices with continuous distributions of the flow quantities. The normalized tangential velocity function $\overline{V_\theta}$ of the Vatistas model is given by $\overline{v} = \frac{v}{\Gamma_\infty/(2\pi r_c)} = \frac{\overline{r}}{(1+\overline{r}^{2n})^{1/n}}$, where $\overline{r} = r/r_c$, r_c is the core radius, v is the tagential velocity, Γ_∞ is the vortex circulation at infinity.

Expermental observations by Vatistas (1986) suggest that in the concentrated vortex the azimuthal velocity component does not depend strongly in the axial direction. Therefore, under these assumptions the radial velocity component can be obtained from the $\theta-$momentum equation, the normalised radial velocity function $\overline{u}$ is given by $\overline{u} = u\frac{r_c}{\nu} = -\{\frac{2(1+n)\overline{r}^{2n-1}}{(1+\overline{r}^{2n})}\}$, where ν is the kinematic viscosity and the normalized axial velocity function $\overline{V_z}$ is given by $\overline{w} = \frac{wz_c}{\nu} = \frac{4n(1+n)\overline{r}^{2n-1}}{(1+\overline{r}^{2n})^2}$, where $\overline{z} = z/r_c$. This approaches Rankine profile as $n \to \infty$. These equations have singularity on the vortex center for $n < 1$. Therefore distribution with for $n < 1$ should not be permitted. For any finite value of n the values of all velocity components are well behaved. The Vatistas (1998) model is a generalization of few

well-known vortex tangential velocity profiles in the aerodynamics community.

Deissler (1977) presented some models to deal with different aspects of atmospheric vertices by considering a single gravity driven vortex and a frictionless adiabatic model. The effects of heat drag, heat transfer and participation induced downdrafts have also been discussed. It is a generalisation of the model given by Deissler (1977) and Boldman (1974). The azimuthal velocity v is supposed to be a function of only radial coordinate r, the axial velocity w depends on z only. The radial velocity u is then computed and found to be dependent on r and z.

Several attempts have been made to model tornadoes. Ward (1956) studied temperature inversion as a factures in the formation of tornadoes. He (1972) later explored certain features of tornado dynamics using a laboratory model. Kuo (1966) studied the dynamics of convective atmospheric vortices. It was followed his (1967) note on the similarity solutions of the vortex equations in an unsteady stratified atmosphere. Bellany-Knights (1970) attempted to get an unsteady two cell solutions of the Navier-Stokes equations. Serrin (1972) modelled a swirling vortex. Lewellen (1993) propounded a detailed tornado vortex theory. Davies-Jones (1995) also discussed tornadoes extensively. Larcheveque and Chaskalovic (1994) discussed tornado genesis and found that the basic flow is generated simultaneously by a strong vertical gradient of temperature and by a storm in the troposphere, which is a non rotating updraft.

Subsequent attempts are their generalisations or investigations of particular aspects following the paths propounded by the authors as described above.

Authors in the most recent reports (Tanamachi et al., 2006; Yih, 2007, Makarieva and Gorshkov, 2009*a*, 2009*b*, 2011; Bestray et al., 2011; Makarieva et al., 2011; Bistray et al., 2011; Arsen'yev, 2011; Bistray and Lykov, 2012; Rotunno, 2013; Davies-Jones, 2015; Ben-Amots, 2016 etc.) have discussed different aspects particularly of tornado like vortex, used different methods or reviewed the literature

extensively.

It is thus observed that intended attempts for modelling a particular type of rotating fluid masses occurring in the atmosphere revolve mainly around tornadoes. Here we intend to model whirlwind mathematically.

3.2 Mathematical formulation of the problem

Dust devils are observed the world over and occasionally throughout the year. These are formed due to temperature gradients created locally due to excessive heating in a locality. This is formed suddenly and is observed to rise into the sky but unlike tornadoes it is short-lived and dies out soon. Even gustnadoes, which, unlike tornadoes, fail to connect with clouds, have very similar characteristics. We intend to model whirlwinds mathematically using a new approach.

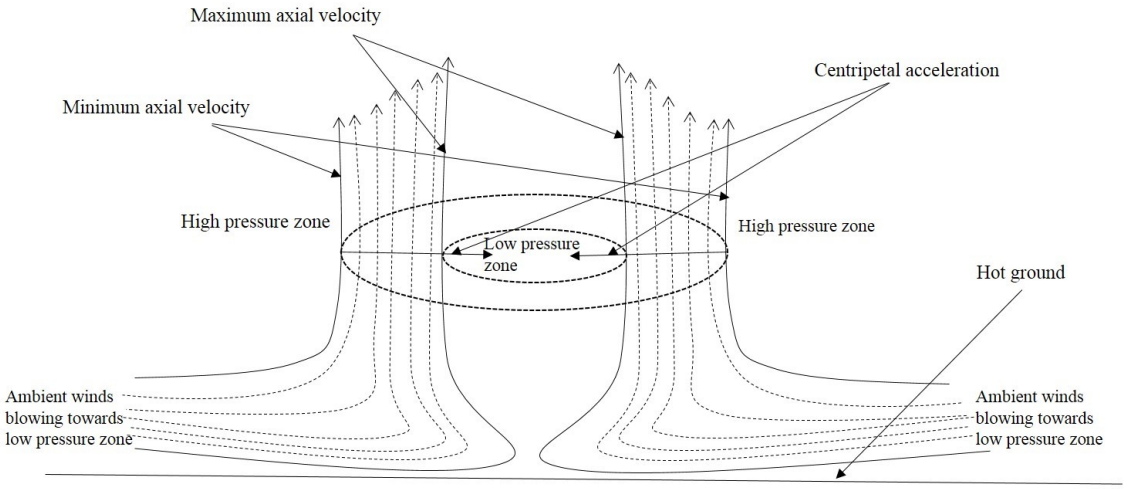

Figure 3.1: Diagrammatic representation of the formation of a dust devil. Dashed curves show the direction of ambient winds blowing horizontally and then moving upward after supressing air the buffer zone, the innermost and the outermost layers being shown by solid curves. Heights of the different layers indicate that the innermost rises the most. The two dotted circles indicate the inner and the outer boundaries of the rotating annular dust devil around a low pressure zone and kept intact by centripetal acceleration.

3.2.1 The physical model of whirlwind vortex

In summer, the sunlight is quite intense. Whenever a particular area of the Earth's surface is exposed to excessive heating, the water contents are evaporated and move upward; the dry and hot air becomes rarer in density and locally creates a void, i.e. a depleted airy zone, forming a horizontal gradient of temperature and air pressure. In order to fill the void, colder winds close to the Earth's surface blow from all the directions and sometimes culminate into the formation of a rotating columnar mass of air mixed with dust, leaves etc., called dust devil. Renno et al. (1998) put forward a thermo-dynamical theory for dust devils explaining how vertical and horizontal temperature gradients are created. Many more detailed descriptions are given by Balme and Greeley (2006). We may use this knowledge but won't dig into it.

The general analysis of fluid motion puts forth the theory of two velocity components, one being normal to a quadric surface and another that is ascribed to rigid body rotation of fluid elements with velocity half the vorticity vector. However, this tendency of rotation is expected to survive only when there exists a central area of lower pressure which helps create centripetal forces in the radial direction. A solid vortex is rare and won't last long as the driving force required to rotate a solid mass in the atmosphere is unusual. Formation of vortex motion in bathtubs is due to water leaving the tub and creating a low pressure zone in the middle. Once exit of water is stopped, the vortex motion calms down.

The strength of the vortex must be dependent on the intensity of the stormy wind, created due to temperature difference, rushing to fill the pressure zone. The layer of the winds closest to the Earth's surface is hottest and so blows fastest;

hence when the winds turn and move vertically upward, the innermost layer must be moving with the highest velocity. This may be used as a boundary condition.

Thus, it may be a cylindrical aerial mass of higher pressure surrounding an inner cylindrical mass of lower pressure. Moments after its birth, it is observed to scale some height suddenly, and soon gets grounded only to die out. This may be possible when a favorable pressure gradient is created for some time in the upward vertical direction or the winds close to the ground have some kinetic energy to take the dust to some height.

The reasons we cite to construct the model are as follows:

The winds rushing from opposite directions and pressed by the following wind compress the air in the buffer zone as much as possible, gradually change the direction of motion due to the reaction of the compressed air and eventually move vertically upward because the atmospheric pressure above it becomes less than the pressure generated due to the compressed air. As a result, a negative pressure gradient is created in the vertically upward direction. Furthermore, the wind in the vicinity of the hot ground has some kinetic energy and the changed direction is along the normal to the ground. The kinetic energy takes the winds to some height by getting converted into potential energy. The rest of the dusty part floating above the whirlwind, which is the debris from the surroundings carried along by the blowing winds, is due to the effects of buoyancy and the electrostatic charges. It is believed that dust storms can generate significant electrostatic fields due to contact between diametrically large and small dust particles. Frictional drag on the air and the electrostatic repulsion owing to electric charge differences between the smaller and the larger dust particles from the triboelectric effect pull up dust in the core. The vertical/horizontal flow has a toroidal vorticity which either lifts the dust and sand directly or balances the downward gravitational force on the sand sufficiently to allow

electro-static forces from triboelectricity to lift the smaller, lighter sand dust into a high rising column (Kok and Renno, 2006). Lacks and Levandovsky (2007) add that saltation, i.e., bouncing of the sand, transfers weakly bound surface electrons from diametrically larger sand particles, particularly SiO_2 to the smaller ones. Further details are given by Horton et al. (2016). These reports endorse our considerations.

The compressed air close to the ground will also move towards the lower pressure zone lying above, travel vertically upward and may in some interval of time annihilate the circumstance that created vortex motion. The height scaled is of a few meters because the velocity with which the winds blow should be enough to take them to a great height. Mattsson et al. (1993) claim them to range from a few meters to 1.0 km. Data reported by Sinclair (1965), Flower (1936) and Williams (1948) suggest that 12 % of the dust devils are lower than 3 meters in height, 50 % range in $3 - 50$ m and only 8 % are taller than 300 m. Some exceptional cases of taller dust devils are also reported (Bell, 1967). The height of the most of the dust devils is found to be at least 5 times their width (Hess and Spillane, 1990). Meanwhile, the winds from all the directions put pressure on the whirlwind and increase its longevity. Sinclair (1966) classified the length of a dust devil into three parts. The lower part being the surface interface region loaded heavily with dust particle, the middle one nearly a vertical column of rotating dust with little exchange of dust between the column and the surrounding air, and the upper one where rotation decays and which expels dust into the ambient atmospheric flow.

The whirlwind also gets drifted. Once the whirlwind drifts and the pressure close to the ground equals the atmospheric pressure, the axial velocity sieges; but the whirlwind may continue rotating due to the azimuthal velocity acquired and radial force being exerted by the winds from the surroundings. But this dragging is

neither a part of the proposed model, nor is it seen as important an issue as rotation at least at this stage of discussion.

Thus, it is likely that such a natural phenomenon is formed by the radial pressure gradient, survives due to the existence of a lower pressure region and is governed by the axial pressure gradient. They are expected to survive as long as the axial pressure gradient continues. The model will help us explore. We attempt to model the middle part of the vortex motion of a dust devil as characterized by Sinclair (1966) using the aforementioned considerations.

3.2.2 Mathematical model of whirlwind vortex

We are modelling the dynamics of whirlwinds as physically described above in mathematical terms as given below:

We consider the cylindrical polar coordinates (r, θ, z) for modelling the problem undertaken, r, θ, z respectively stand for radial, angular and axial coordinates. Simplifications are incorporated in the general governing equations in order to get conformance with the physical model as explained below step-by-step.

It is observed that at least practically, a rotating fluid mass in the form of a vortex does not seem to differ at different angles during its rotation about the vertical axis. Thus, it seems reasonable to consider the flow as axi-symmetric. This removes all terms where the angular coordinate θ is involved. Hence, the three-dimensional Navier-Stokes governing equations for the steady axi-symmetric flow of an incompressible Newtonian viscous fluid may be given by

$$u\frac{\partial u}{\partial r} + w\frac{\partial u}{\partial z} - \frac{v^2}{r} = -\frac{1}{\rho}\frac{\partial p}{\partial r} + \nu\left\{\frac{\partial^2 u}{\partial r^2} + \frac{1}{r}\frac{\partial u}{\partial r} - \frac{u}{r^2} + \frac{\partial^2 u}{\partial z^2}\right\}, \tag{3.1}$$

$$u\frac{\partial v}{\partial r} + w\frac{\partial v}{\partial z} + \frac{uv}{r} = \nu\left\{\frac{\partial^2 v}{\partial r^2} + \frac{1}{r}\frac{\partial v}{\partial r} - \frac{v}{r^2} + \frac{\partial^2 v}{\partial z^2}\right\}, \tag{3.2}$$

$$u\frac{\partial w}{\partial r} + w\frac{\partial w}{\partial z} = -\frac{1}{\rho}\frac{\partial p}{\partial z} + b + \nu\left\{\frac{\partial^2 w}{\partial r^2} + \frac{1}{r}\frac{\partial w}{\partial r} + \frac{\partial^2 w}{\partial z^2}\right\}, \tag{3.3}$$

together with the continuity equation

$$\frac{1}{r}\frac{\partial (ru)}{\partial r} + \frac{\partial w}{\partial z} = 0. \tag{3.4}$$

where r and z are cylindrical polar coordinates; and u, v and w are the radial, azimuthal and axial components of velocity vectorand, b is buoyancy.

For modelling a vortex mathematically, which spins vertically and is made up of an incompressible fluid, i.e., the density ρ remains constant, we consider the flow to be steady, i.e., it does not change with time. Practically, radial velocity is insignificant once the whirlwind is fully developed, i.e., the middle part as classified by Sinclair (1966). Hence is the assumption $u = 0$. The effect of buoyancy is significant for the upper part of a dust devil which has decayed rotation and floating dust particles; therefore we set $b = 0$. The simplest case is that the azimuthal velocity is described in terms of an angular frequency or velocity ω. We suppose that the angular velocities of the innermost and outermost layers are ω_i and ω_o respectively. Thus, the azimuthal velocities of the innermost and outermost layers are described respectively as $v_i = \omega_i r_i$ and $v_o = \omega_o r_o$, ω_i and ω_o being respectively the innermost and outermost angular velocities. The radial velocity is still considered as zero, i.e. $u = 0$. Under the assumptions described above, the modified boundary equations are as follows:

$$\omega_i = \omega\left(r_i\right),\ \omega_o = \omega\left(r_o\right), \tag{3.5}$$

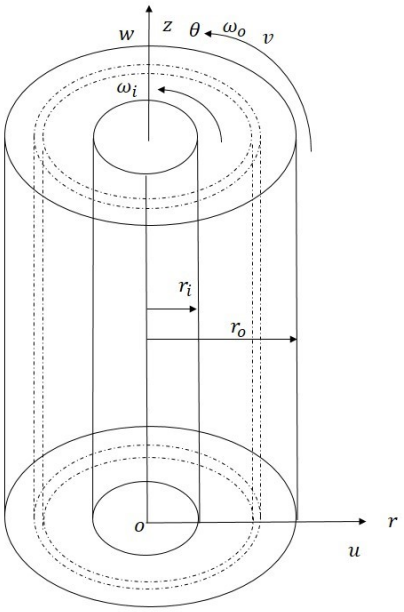

Figure 3.2: The diagram gives the geometry of the whirlwind modelled as an annulus, drawn by solid lines and curves, of outermost radius r_o and innermost radius r_i measured from the axis oz. The inner region of radius r_i inside the annulus is a region of low pressure. The annulus is filled with air and has comparatively high pressure. Inside the annulus are shown concentric cylindrical layers shown by dotted lines, differing in some respect. u, v and w represent the radial, the azimuthal and the axial velocities respectively and ω_i and ω_o are respectively the angular velocities of the innermost and the outermost surfaces of the annulus.

A whirlwind is a vertical circularly rotating fluid mass. We model this as a cylindrical annulus of dense aerial mass, inside which lies a region of an aerial mass of low pressure, thus creating a favourable radial gradient of pressure (cf Fig. 3.1). Thus, there are two concentric vertical cylindrical surfaces, say innermost and outermost surfaces. The annular mass has concentric cylindrical forms rotating with varying azimuthal velocities.

It is practically observed that the innermost part of a dust devil reaches the top height. That is, the innermost part, which is in contact with the low pressure region, rotate and move vertically with the highest axial velocity. Hence, there is

nothing wrong in the assumption that the maximum axial velocity is achieved at the innermost surface of the annular cylindrical mass. If we move towards the outermost surface, we find that the concentric layers slow down and the axial velocity of the outermost layer is minimum and asymptotically maybe even zero. We believe that the distance is practically finite, say r_o from the axis oz.

In view of the assumption that $u = 0$, the continuity Eq. (3.4) reduces to $\partial w/\partial z = 0$, and yields the axial velocity which is independent of the axial coordinate, i.e. $w = w(r)$. Taking this revelation into consideration, Eqs. (3.1) and (3.3) may be presented for the steady flow, in reduced form, as

$$\frac{v^2}{r} = \frac{1}{\rho}\frac{\partial p}{\partial r}, \tag{3.6}$$

$$\frac{1}{\rho}\frac{\partial p}{\partial z} = \nu\left\{\frac{\partial^2 w}{\partial r^2} + \frac{1}{r}\frac{\partial w}{\partial r}\right\}, \tag{3.7}$$

It is noticed that Eq. (3.6) describes the centripetal acceleration.

In fact, the mutual frictional/viscous forces acting between consecutive layers diminish velocity and as a consequence, the highest part of the whirlwind is seen to be surrounded by spinning wind of lesser height which is itself surrounded by unmoved air. Under this consideration, the axial velocity is derived from Eq. (3.7) under the boundary conditions

$$w(r_o) = 0 \text{ and } w(r_i) = w_{max}, \text{ (maximum axial velocity)}\ , \tag{3.8}$$

Since $w(r)$ does not depend on z, it is evident from Eq. (3.7) that the right side of the equality sign is a function of r only. As a consequence, $\partial p/\partial z$ is either a function of r or is a constant or both the sides are equal to a constant. Later we shall see in Eq. (3.17) that though p is a function of r and z both but not a product of them or

their functions, therefore it is merely a constant. Hence, integrating Eq. (3.7) under the condition that $w(r_o) = w_o$, we get

$$w(r) = w_o + \frac{P}{2\mu}\left(\frac{r^2 - r_o^2}{2}\right) + K \times \log_e\left(\frac{r}{r_o}\right), \tag{3.9}$$

where the axial pressure gradient, $\partial p/\partial z = P$, a constant and K is a constant of integration required to be evaluated for $w(r_i) = w_{max}$. Maximisation of the axial velocity gives $K = -\frac{P}{2\mu}r_i^2$, so that,

$$w(r) = w_o - \frac{P}{2\mu}\left(\frac{r_o^2 - r^2}{2} + r_i^2 \times \log_e\left(\frac{r}{r_o}\right)\right), \tag{3.10}$$

The kinetic energy $\rho w_{initial}^2(r)/2$ due to the initial velocity $w_{initial}(r)$ of the wind can take it to some height $h(r) = w_{initial}^2(r)/2g$; and hence it may be added to the right side of Eq. (3.10), so that

$$w(r) = w_o + \sqrt{2gh(r)} - \frac{P}{2\mu}\left(\frac{r_o^2 - r^2}{2} + r_i^2 \times \log_e\left(\frac{r}{r_o}\right)\right), \tag{3.11}$$

In the absence of the logarithmic term, the axial velocity, given by Eq. (3.10), reduces to Hagan-Poiseuille flow. The logarithmic term appears due to the assumption that the axial velocity is maximum at the inner radius while in the Hagan-Poiseuille flow, the inner radius is zero. This is notable that this model is valid only when the axial pressure gradient is constant. Once the axial pressure gradient changes, this no longer holds. After a particular height, change in pressure gradient is not ruled out; and so the model governing the flow will also change. Due to the velocity, normal to the quadric surface, the vortex keeps drifting; and consequently it probably reaches a place with pressure gradient inadequate to sustain the vortex.

The modification brought about in this case is that the angular velocities

of the innermost and the outermost layers are supposed to be ω_i and ω_o respectively. Thus, the innermost and outermost layer azimuthal velocities are described respectively as $v_i = \omega_i r_i$ and $v_o = \omega_o r_o$, where ω_i and ω_o being respectively the innermost and outermost angular velocities. The radial velocity is still considered as zero, i.e. $u = 0$. Under the assumptions described above, the modified boundary equations are as follows:

$$\omega_i = \omega\left(r_i\right), \ \omega_o = \omega\left(r_o\right), \tag{3.12}$$

In view of the varying azimuthal velocity, Eq. (3.2) reduces to

$$\frac{\partial^2 v}{\partial r^2} + \frac{1}{r}\frac{\partial v}{\partial r} - \frac{v}{r^2} = 0, \tag{3.13}$$

which is homogeneous Euler-Cauchy's equation with the following solution:

$$v(r) = Ar + \frac{B}{r} \tag{3.14}$$

where A, B are arbitrary constants of integration.

Under the boundary conditions (3.12), Eq. (3.14), in terms of angular velocity, is of the form

$$\omega\left(r\right) = \frac{r_o^2}{r_o^2 - r_i^2}\left[\omega_i\left(\frac{r_o^2 - r_i^2}{r_o^2} - \frac{r^2 - r_i^2}{r^2}\right) + \omega_o\left(\frac{r^2 - r_i^2}{r^2}\right)\right]. \tag{3.15}$$

This is standard Couette flow.

Hence, the flow of the vortex thus created may be given, in the consolidated form,

by

$$\left.\begin{aligned} u(r) &= 0, \\ v(r) = r\omega\left(r\right) &= \frac{1}{r_o^2 - r_i^2}\left[\left(\omega_o r_o^2 - \omega_i r_i^2\right) r - \left(\omega_o - \omega_i\right)\frac{r_i^2 r_o^2}{r}\right], \\ w(r) &= w_o + \sqrt{2gh(r)} - \frac{P}{2\mu}\left(\frac{r_o^2 - r^2}{2} + r_i^2 \times \log_e\left(\frac{r}{r_o}\right)\right). \end{aligned}\right\} \tag{3.16}$$

The corresponding vorticity vector is given by

$$\boldsymbol{\zeta} = \hat{\boldsymbol{r}}0 + \hat{\boldsymbol{\theta}}\frac{P}{2\mu}\left(\frac{r_i^2}{r} - r\right) + \hat{\boldsymbol{z}}\frac{2\left(\omega_o r_o^2 - \omega_i r_i^2\right)}{r_o^2 - r_i^2}, \tag{3.17}$$

where $\boldsymbol{\zeta}$, $\hat{\boldsymbol{r}}$, $\hat{\boldsymbol{\theta}}$, $\hat{\boldsymbol{z}}$ are respectively vorticity vector and unit vectors along the radial, azimuthal and axial directions.

The models presented by Rankine (1882), Oseen (1912), Taylor's (1918) model and Lamb (1932) do not describe any axial fluid motion despite the fact that the azimuthal velocity have more general and complex expressions representing more general forms of azimuthal velocity. Hence, those models are not suitable for a vortex model describing the motion of dust devil.

For $\omega_o = \omega_i = \omega$, the flow described in set of Eqs. (3.16), will reduce to

$$\left.\begin{aligned} u(r) &= 0, \\ v(r) &= r\omega, \\ w(r) &= w_o + \sqrt{2gh(r)} - \frac{P}{2\mu}\left(\frac{r_o^2 - r^2}{2} + r_i^2 \times \log_e\left(\frac{r}{r_o}\right)\right). \end{aligned}\right\} \tag{3.18}$$

In view of the angular velocity given by Eq. (3.15) together with Eq. (3.6), the radial pressure gradient will take the following form:

$$\frac{\partial p}{\partial r} = r\rho\left(\frac{r_o^2}{r_o^2 - r_i^2}\right)^2\left[\omega_i r_i^2\left(\frac{1}{r^2} - \frac{1}{r_o^2}\right) + \omega_o\left(1 - \frac{r_i^2}{r^2}\right)\right]^2, \tag{3.19}$$

Integrating Eq. (3.19) with respect to r, the pressure is given by

$$p(r,z) = f(z) + \rho\left[\omega_i\left(\omega_i\frac{r^2}{2} - (\omega_i-\omega_o)\frac{2r_o^2}{r_o^2-r_i^2}\left(\frac{r^2}{2} - r_i^2\log_e r\right)\right)\right. \\ \left. + (\omega_i-\omega_o)^2\left(\frac{r_o^2}{r_o^2-r_i^2}\right)^2\left(\frac{r^2}{2} - 2r_i^2\log_e r - \frac{r_i^4}{2r^2}\right)\right], \tag{3.20}$$

where $f(z)$ is a function of z. Evaluating the pressure at $r = r_i$, we get

$$p(r,z) = p(r_i,z) + \rho\left[\omega_i\left(\omega_i\frac{r^2-r_i^2}{2} - (\omega_i-\omega_o)\frac{2r_o^2}{r_o^2-r_i^2}\left(\frac{r^2-r_i^2}{2} - r_i^2\log_e\left(\frac{r}{r_i}\right)\right)\right)\right. \\ \left. + (\omega_i-\omega_o)^2\left(\frac{r_o^2}{r_o^2-r_i^2}\right)^2\left(\frac{r^2-r_i^2}{2} - 2r_i^2\log_e\left(\frac{r}{r_i}\right) + \frac{r_i^2(r^2-r_i^2)}{2r^2}\right)\right], \tag{3.21}$$

If we evaluate the pressure at $r = r_o$ using Eq. (3.20), we get

$$p(r,z) = p(r_o,z) - \rho\left[\omega_i\left(\omega_i\frac{r_o^2-r^2}{2} - (\omega_i-\omega_o)\frac{2r_o^2}{r_o^2-r_i^2}\left(\frac{r_o^2-r^2}{2} - r_i^2\log_e\left(\frac{r_o}{r}\right)\right)\right)\right. \\ \left. + (\omega_i-\omega_o)^2\left(\frac{r_o^2}{r_o^2-r_i^2}\right)^2\left(\frac{r_o^2-r^2}{2} - 2r_i^2\log_e\left(\frac{r_o}{r}\right) + \frac{r_i^4}{2}\left(\frac{1}{r^2} - \frac{1}{r_o^2}\right)\right)\right], \tag{3.22}$$

The pressure across the width of the whirlwind may therefore be given, by subtracting Eq. (3.22) from Eq. (3.21), as

$$p(r_o,z) - p(r_i,z) = \rho\left[\omega_i\left(\omega_i\frac{r_o^2-r_i^2}{2} - (\omega_i-\omega_o)\frac{2r_o^2}{r_o^2-r_i^2}\left(\frac{r_o^2-r_i^2}{2} - r_i^2\log_e\left(\frac{r_o}{r_i}\right)\right)\right)\right. \\ + (\omega_i-\omega_o)^2\left(\frac{r_o^2}{r_o^2-r_i^2}\right)^2\left(\frac{r_o^2-r_i^2}{2} - 2r_i^2\log_e\left(\frac{r_o}{r_i}\right)\right. \\ \left.\left. + \frac{r_i^2}{2}\left(1 - \frac{r_i^2}{r_o^2}\right)\right)\right], \tag{3.23}$$

under the assumption that the axial pressure gradient, $\partial p/\partial z = P$, is a constant, the axial velocity is the same as Eq. (3.11).

For $\omega_i = \omega_o = \omega$, Eq. (3.21) and Eq. (3.22) give

$$p\left(r,z\right) = p\left(r_i,z\right) + \frac{\rho\omega^2\left(r^2 - r_i^2\right)}{2}, \tag{3.24}$$

or equivalently,

$$p\left(r,z\right) = p\left(r_o,z\right) - \frac{\rho\omega^2\left(r_o^2 - r^2\right)}{2}, \tag{3.25}$$

The pressure across the two layers, in view of Eq. (3.24) and Eq. (3.25) may be given by

$$p\left(r_o,z\right) - p\left(r_i,z\right) = \frac{\rho\omega^2\left(r_o^2 - r_i^2\right)}{2} > 0. \tag{3.26}$$

3.3 Discussions and physical interpretations

Unlike earlier models, in which the axial velocity was considered either zero or of a definite form and subsequently the azimuthal velocity was deduced, we considered the azimuthal velocity of a particular form and tried to work out the axial velocity for physical models resembling whirlwinds, particularly dust devils, occurring in the nature.

3.3.1 Axial velocity vs. radius

A whirlwind is observed to shoot up into the sky immediately after it is born. It is clear from Eq. (3.11) that surging up into the sky is possible only when the winds move upward with some initial velocity or there is a favourable pressure gradient in the axial direction or both. Absence of both will let the whirlwind siege its growth.

For the present analysis and discussion based on numerical solutions, we consider the axial velocity of the outermost layer $w_0 = 0$ and further do not consider the contribution made by the initial winds' velocities $\sqrt{2gh(r)}$.

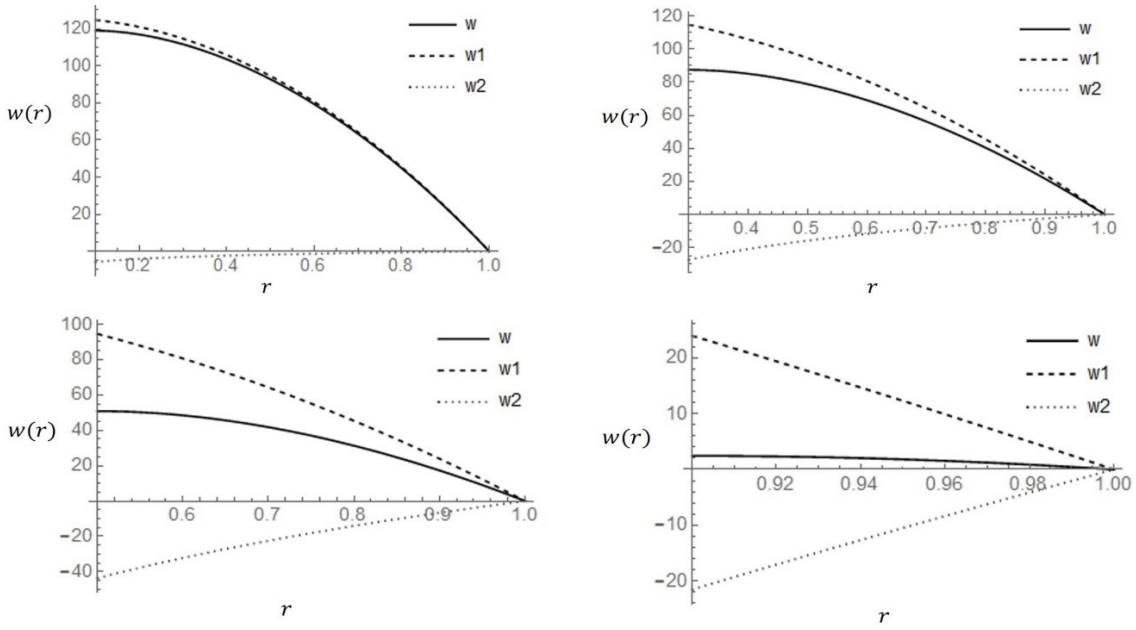

Figure 3.3: The diagrams $(a-d)$ represent the variation of axial velocity $w(r)$ with respect to radius, $w(r)$ has been given by Eq. (3.11) as a sum of w_0, w_1 and w_2, where $w_0 = 0$, $w_1 = -P\left(r_o^2 - r^2\right)/4\mu$ and $w_2 = -Pr_i^2 \log_e\left(\frac{r}{r_o}\right)/2\mu$ as described in the discussion. w_1 and w_2, are separately plotted and later as a sum $w(r)$. The outer radius is $r_o = 1.0\ m$, (a) $r_i = 0.1\ m$, (b) $r_i = 0.3\ m$, (c) $r_i = 0.5\ m$ and (d) $r_i = 0.9\ m$. Other parameters used here are: dynamic viscosity $\mu = 0.0000198\ Pl$, and $P = -0.01\ Pa/m$.

Axial velocity, $w\,(r)$ given by Eq. (3.11) has two parts $-\frac{P}{2\mu} \times \left(\frac{r_o^2 - r^2}{2}\right)$, say $w_1\,(r)$ and $-\frac{P}{2\mu} r_i^2 \log_e\left(\frac{r}{r_o}\right)$, say $w_2\,(r)$. The former part $w_1\,(r)$, which has parabolic profile, gives the main contribution to the axial velocity while the latter part $w_2\,(r)$, which is also parabolic, reduces the magnitude of the axial velocity. This is because under the consideration of favourable pressure gradient, i.e. $P < 0$, we have $\log_e\left(\frac{r}{r_o}\right) < 0$ for $r_i < r < r_o$. This is also revealed through the Fig. 3.2$(a-d)$ plotted for r vs. $w\,(r)$.

The dynamic viscosity, $\mu = 0.0000198\ Pl$ is reported in the literature. We set the outermost radius as $r_o = 1\ m$ (based on the reports by Hess and Spillane, 1990; Flower, 1936 and Williams, 1948) and vary the innermost radius r_i in the range $0.1\ m - 0.9\ m$. The axial pressure gradient is assumed to be $-0.01\ Pa/m$ for the plots. Graphs are plotted by varying inner radius and depicted through Fig. 3.3$(a-d)$. Inside the region within the innermost radius, there is no axial velocity. It varies between the innermost and the outermost radii. The resultant velocity $w(r)$ is less than that of the first part i.e. $w_1(r)$. This gives rise to curiosity about the role the second part, i.e. $w_1(r)$, plays. The investigation follows.

This is observed through Fig. 3.3$(a-d)$ that the axial velocity reduces as the innermost radius r_i is increased. The part of the expression for the axial velocity contributing negatively, denoted by $w_2(r)$, also increases in magnitude; and hence the total sum is further reduced. For $r_i = 0.9\ m$ with $r_0 = 1\ m$, the axial velocity $w(r)$ is very much reduced. This may be concluded that the whirlwind can scale a good height only when the annulus thus formed is thick. We name it inference-1.

We further observe that the axial velocity componen $\log_e\left(\frac{r}{r_o}\right)$ is negative for the entire range $r_i < r < r_o$, and $\log_e\left(\frac{r}{r_o}\right) \to -\infty$ as $r_i \to 0$. This is also observed that r_i and $|w_2(r)|$ decrease simultaneously; and $w_2(r) \to 0$ as $r_i \to 0$. This leads to the conclusion that in the limiting case $r_i \to 0$, the axial velocity is maximum. This we name inference$-II$.

Further, for $r_i < r < r_o$, we have $w(r) \to -P\left(r_o^2 - r^2\right)/4\mu\,(= w_1(r))$ as $r_i \to 0$. Hence, the latter part $w_2(r)$ of the axial velocity $w(r)$ is due to the inner region of low pressure of the whirlwind. The second part $w_2(r)$ of the axial velocity $w(r)$ thus plays a vital role in the whirlwind dynamics as predicted by the model and it characterises, in fact, all the phenomena similar to whirlwinds.

3.3.2 Azimuthal velocity vs. radius

Due to the frictional forces acting between consecutive layers, the velocity of the outer layer is evidently less. It is observed that the maximum angular velocity of a whirlwind occurring in the nature is found at the innermost radius. Taking this fact into consideration, we go ahead with further discussions.

It is evident from the Eq. (3.6) that absence of radial pressure gradient $\partial p/\partial r = \omega^2 r$ is possible when either the angular velocity ω or the radial length r is zero. In either of the cases, the whirlwind will die out. Thus, it may be predicted that the moment the low pressure region disappears, the whirlwind will vanish. Hence, the inner radius, r_i is never zero and consequently, $r \not\to 0$, at the most $r \to r_i\,(\neq 0)$. This may be physically interpreted that a whirlwind with no low pressure region inside it cannot survive. Thus, this may be regarded as the fundamental characteristic.

Inference$-II$ together with the fundamental characteristic leads to the conclusion that that the axial velocity of the innermost layer increases but $\omega(r_i) \to 0$ when the inner radius $r_i \to 0$. Thus, in such a case the whirlwind attains the maximum axial velocity and then dies out. This is practically observed.

The characteristics discussed above have never been under investigation for any of the models available in the literature. Models not considering vertical velocity cannot represent whirlwinds that surge up into the sky. The Burgers (1940, 1948) models predict a linearly increasing vertical velocity which is not realistic and unacceptable for dust devils that surge up into the sky and die out in a short while.

With more realistic and experimentally verified considerations of radial and azimuthal velocities, it is possible to predict more useful results following the methodology involved in this model. This is worth mentioning that if we artificially

create these circumstances using concentrated sun energy, stationed whirlwinds may be created which may facilitate us generate electric power for domestic and industrial consumptions.

The azimuthal velocity in this model is dependent on three factors, namely, the radius and the inner and outer angular velocities. In order to study their effects, three sets of Figs. (3.4–3.6) have been drawn which exhibit how the angular and azimuthal velocities depend on the radial distance; and further what impacts the changes in the inner and outer angular velocities give.

Balme and Greeley (2006) summarised the various reports available on the velocities etc. of dust devils. The values for the discussion are more or less based on them. In Fig. 3.4$(a-d)$, the outer and inner angular velocities are set as $\omega_o = 20\ cycles\ s^{-1}$, and $\omega_i = 25\ cycles\ s^{-1}$ and the innermost radius is varied in the range $r_i = 0.1\ m - 0.9\ m$. As expected, the angular velocity decreases as we move outward along the radius. In Fig. 3.4, where the two angular velocities are close in magnitude, it is observed that the azimuthal velocity, however, increases along the radius in the outward direction when the innermost radius is small. But when the innermost radius is very large, i.e., the whirlwind is quite thin, the azimuthal velocity, too, starts decreasing along with the angular velocity as we move outward along the radius.

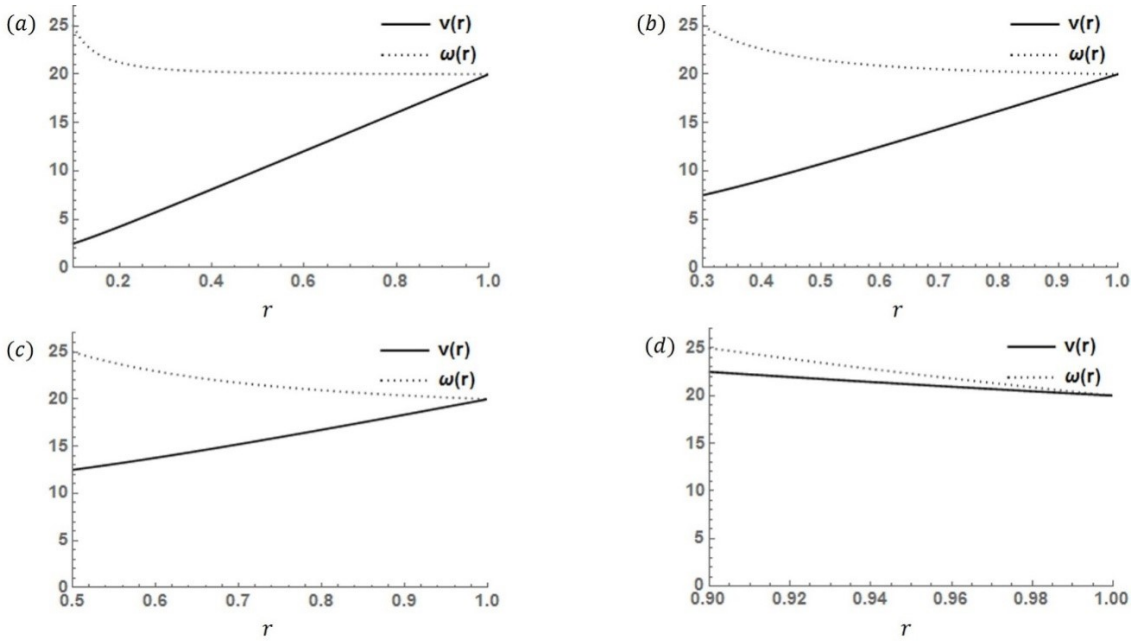

Figure 3.4: The diagrams $(a-d)$ represent the variation of angular velocity and corresponding azimuthal velocity with radius based on Eq. (3.15). Here the angular velocities are fixed as $\omega_o = 20\ cycles\ s^{-1}$, and $\omega_i = 25\ cycles\ s^{-1}$, the outer radius is set as $r_o = 1.0\ m$ while the inner radius has been varied in the range $r_i = 0.1\ m - 0.9\ m$.

In Fig. 3.5$(a-d)$, the angular velocities are fixed as $\omega_o = 5\ cycles\ s^{-1}$, and $\omega_i = 25\ cycles\ s^{-1}$, the outermost radius is set as $r_o = 1.0\ m$ while the innermost radius has been varied in the range $r_i = 0.1\ m - 0.9\ m$. In Fig. 3.4, where the two angular velocities differ largely in magnitude, it is observed that the azimuthal velocity increases along the radius in the outward direction when the inner radius is very small. But when the inner radius is somewhat larger, i.e., the whirlwind is still thick, the azimuthal velocity, too, starts decreasing along with the angular velocity as we move outward along the radius.

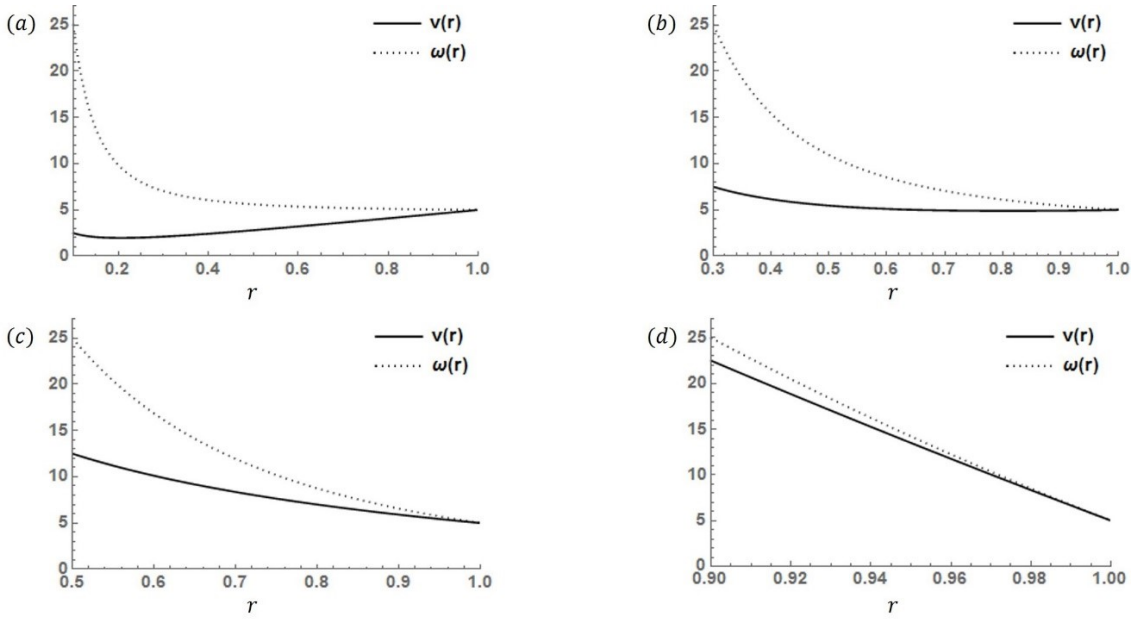

Figure 3.5: The diagrams $(a-d)$ display the variation of angular velocity and corresponding azimuthal velocity with radius based on Eq. (3.15). The various parameters used for the plots are: $\omega_o = 5\ cycles\ s^{-1}$, $\omega_i = 25\ cycles\ s^{-1}$, $r_o = 1.0\ m$, $r_i = 0.1\ m - 0.9\ m$.

In Fig. 3.6$(a-d)$, we consider no outer angular velocity. The inner angular velocity is fixed as $\omega_i = 25\ cycles\ s^{-1}$, the outer radius is set as $r_o = 1.0\ m$ while the innermost radius has been varied once again in the range $r_i = 0.1\ m - 0.9\ m$. In Fig. 3.6, in which the outer angular velocity is set to zero, the angular and azimuthal velocities decrease simultaneously as we move outward along the radius.

One can conclude from this that it is not the magnitude of azimuthal velocity but that of angular velocity which determines motion of a vortex. Thus, a fundamental parameter for such a fluid motion is the angular velocity and not the azimuthal velocity.

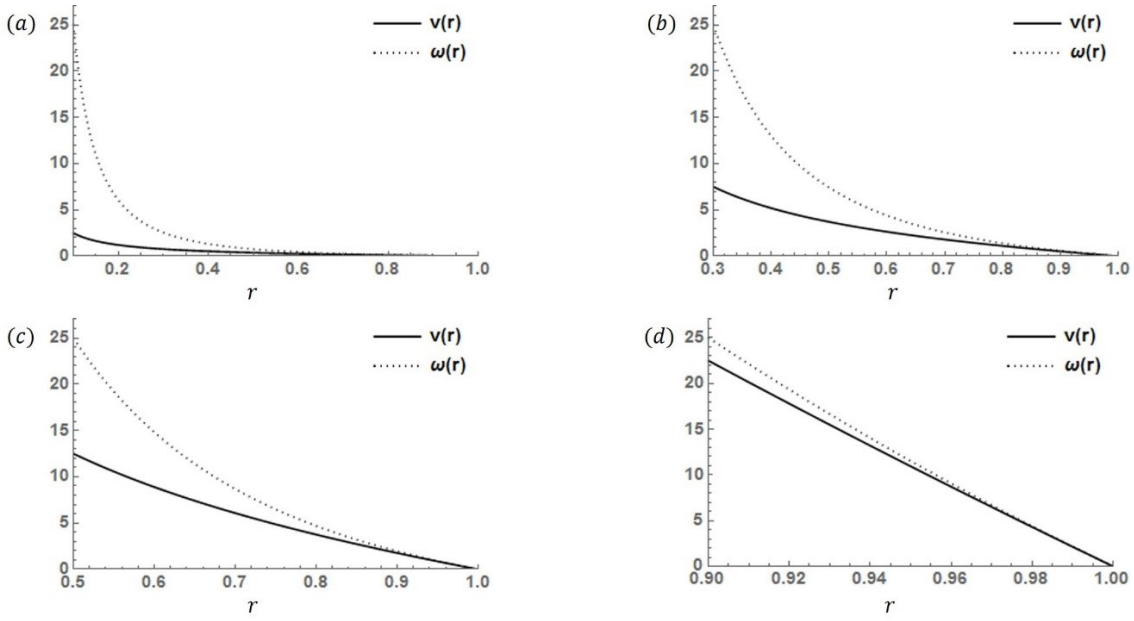

Figure 3.6: The diagrams $(a-d)$ display the variation of angular velocity and corresponding azimuthal velocity with radius based on Eq. (3.15). The various parameters used for the plots are: $\omega_o = 0$ *cycles* s^{-1}, $\omega_i = 25$ *cycles* s^{-1}, $r_o = 1.0\ m$, $r_i = 0.1\ m - 0.9\ m$.

3.3.3 Pressure vs. radius

We plot graphs, given in Figs. (3.7–3.9), for $p\,(r,z) - p\,(r_i,z)$ vs. r, $r_i \leq r \leq 1$, under the consideration that $\omega_o = 0$ *cycles* s^{-1}, and $\omega_i = 25$ *cycles* s^{-1}. It is observed that pressure rises very sharp in the vicinity of the innermost radius but then relaxes and rises very slowly and near the outer boundary, the pressure rise seems to be almost zero. A similar pattern is observed when we use Eq. (3.22). To avoid unnecessary repetition, we do not include those graphs here.

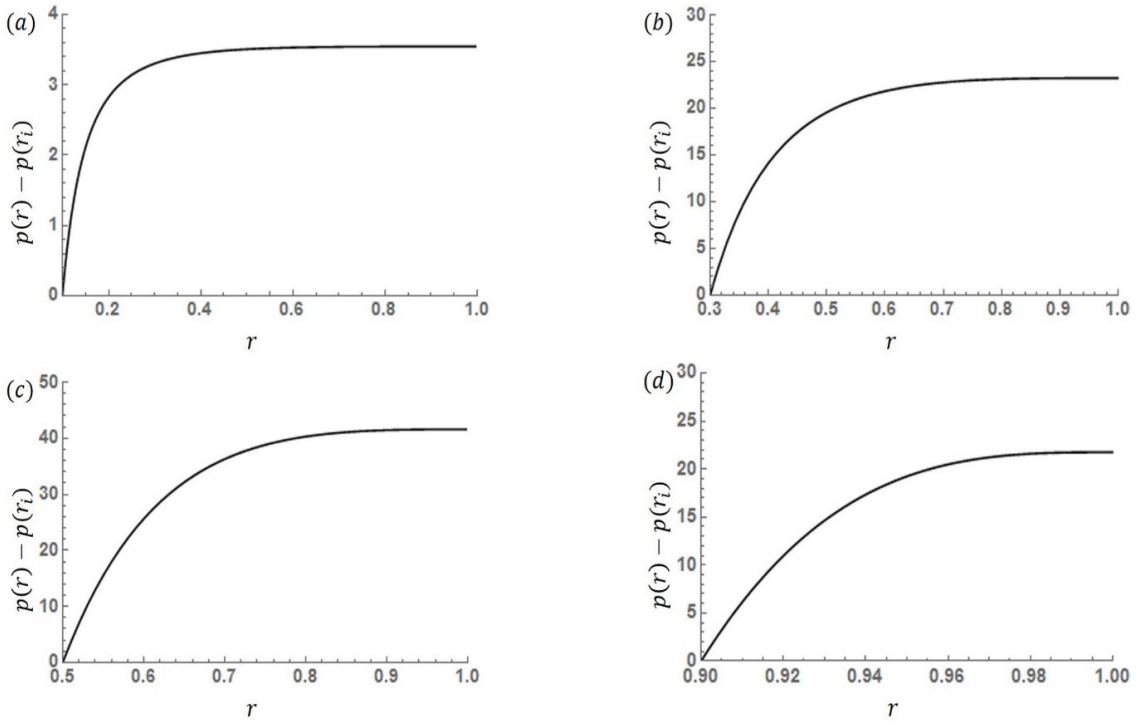

Figure 3.7: The diagrams $(a-d)$ represent the variation of pressure difference with radius. This is based on Eq. (3.21). This corresponds to $\omega_o = 0\ cycles\ s^{-1}$, and $\omega_i = 25\ cycles\ s^{-1}$. In the four cases the inner radius varies as $(a)\ r_i = 0.1\ m$, $(b)\ r_i = 0.3\ m$, $(c)\ r_i = 0.5\ m$, $(d)\ r_i = 0.9\ m$.

Similar graphs we plot under the consideration that $\omega_o = 5\ cycles\ s^{-1}$, and $\omega_i = 25\ cycles\ s^{-1}$. The difference observed is that when the innermost radius is very small for example, $r = 0.1\ m$, the pressure rises in the close vicinity of the inner radius but does not slow down rapidly, it rather once again increases a bit. This is confirmed by plotting graphs for pressure gradient shown in Fig. 3.9$(a-d)$.

We further increase the outer angular velocity and set $\omega_o = 20\ cycles\ s^{-1}$, so that it is close to the inner one. In this case, the pressure increases right from the beginning.

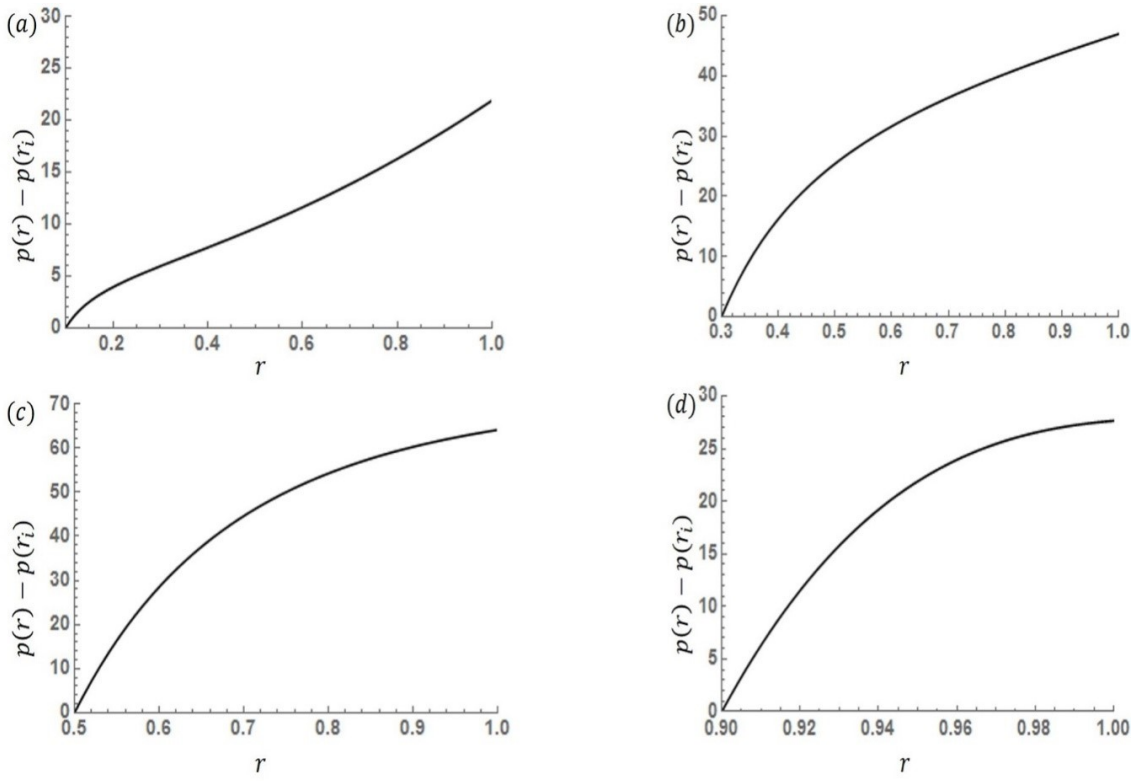

Figure 3.8: The diagrams $(a - d)$ represent the variation of pressure difference with radius. This is based on Eq. (3.21). This corresponds to $\omega_o = 5\ cycles\ s^{-1}$, and $\omega_i = 25\ cycles\ s^{-1}$. In the four cases the inner radius varies as $(a)\ r_i = 0.1\ m$, $(b)\ r_i = 0.3\ m$, $(c)\ r_i = 0.5\ m$, $(d)\ r_i = 0.9\ m$.

From the above discussion, it is inferred that pressure increases from the innermost to the outermost layer; and if the two angular veocities are close in magnitude, the pressure gradient increses towards the outermost layer but if the two angular velocities are farther in magnitude, the pressure gradient near the innermost layer is very large and decreases at a fast rate as we move towards the outermost layer.

Finally, we draw diagrams for 'pressure across the whirlwind width' vs. the innermost radius given through the Figs. (3.10−3.12) based on Eq. (3.23). Through the Fig. 3.10$(a - d)$, it is observed that, when the difference in the magnitudes of the two angular velocities is large (e.g., $\omega_o = 0\ cycles\ s^{-1}$, and $\omega_i = 25\ cycles\ s^{-1}$),

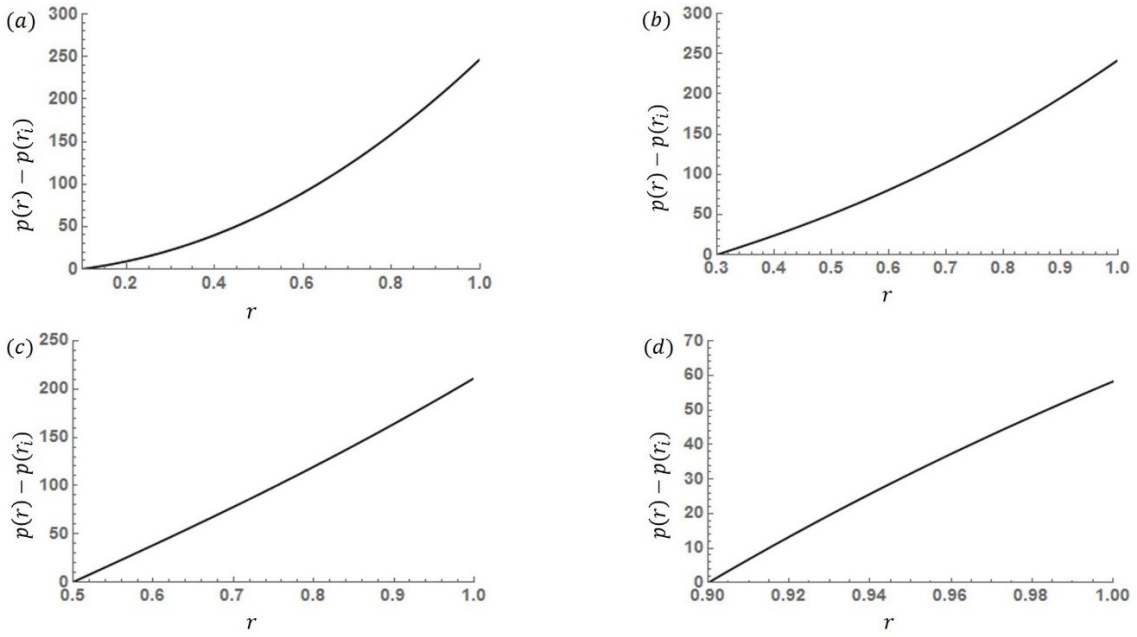

Figure 3.9: The diagrams $(a-d)$ represent the variation of pressure difference with radius. This is based on Eq. (3.21). This corresponds to $\omega_o = 20\ cycles\ s^{-1}$, and $\omega_i = 25\ cycles\ s^{-1}$. In the four cases the inner radius varies as $(a)\ r_i = 0.1\ m$, $(b)\ r_i = 0.3\ m$, $(c)\ r_i = 0.5\ m$, $(d)\ r_i = 0.9\ m$.

two different values of the inner radius correspond to the same pressure except a particular case when the pressure is the maximum. But if the whirlwind is thin, the pressure across the two layers decreases if the inner radius increases.

We diminish the difference in the magnitudes of the two angular velocities taking $\omega_o = 5\ cycles\ s^{-1}$, and $\omega_i = 25\ cycles\ s^{-1}$, the maximum pressure increases which corresponds to only one value of the inner radius (see Fig. 3.11$(a-d)$).

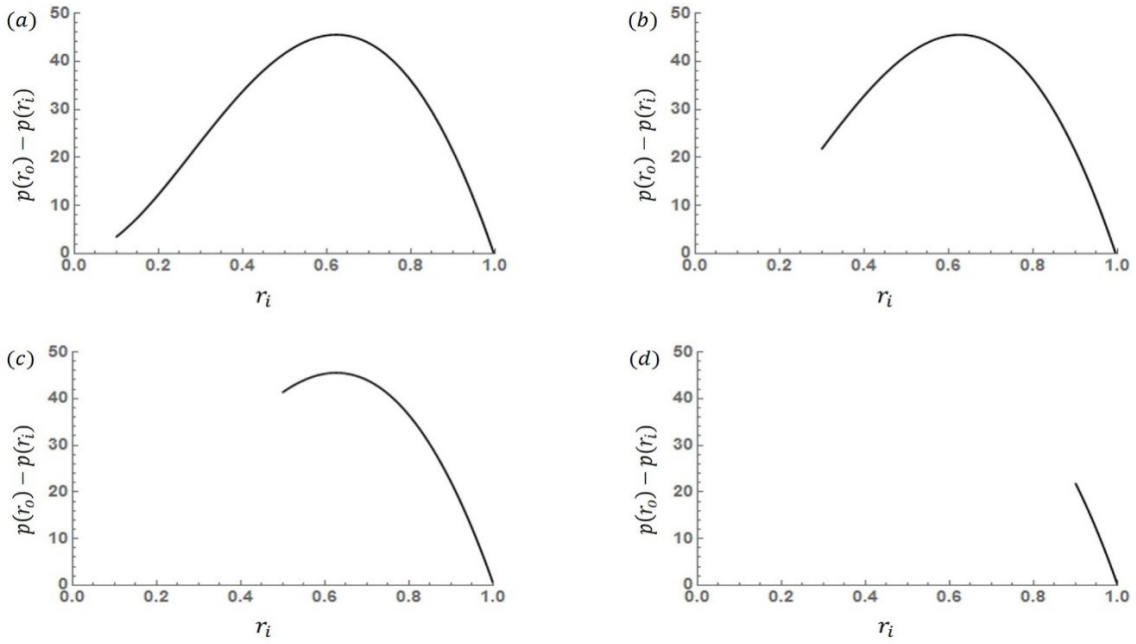

Figure 3.10: The diagrams $(a - d)$ exhibit the variation of pressure difference across the innermost and the outermost layers with inner radius. This is based on Eq. (3.23). This corresponds to $\omega_o = 0$ *cycles* s^{-1}, and $\omega_i = 25$ *cycles* s^{-1}. In the four cases the inner radius varies as (a) $r_i = 0.1$ m, (b) $r_i = 0.3$ m, (c) $r_i = 0.5$ m, (d) $r_i = 0.9$ m.

But when the difference further decreased with $\omega_o = 20$ *cycles* s^{-1}, and $\omega_i = 25$ *cycles* s^{-1}, the pressure across the two layers decreases with increasing inner radius (see Fig. 3.12$(a - d)$).

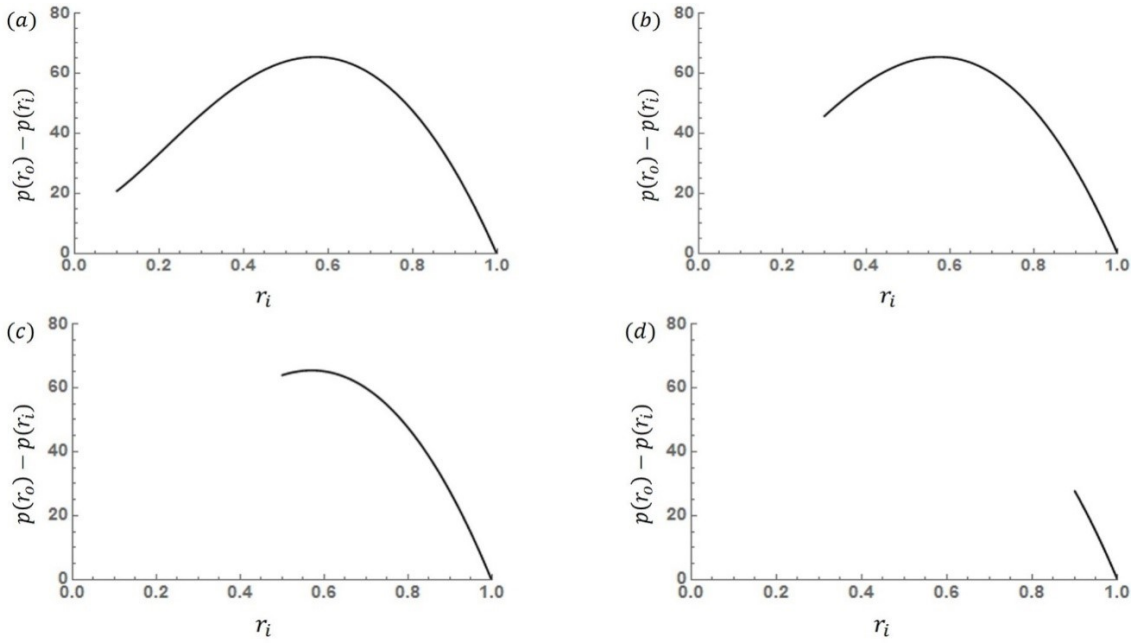

Figure 3.11: The diagrams $(a - d)$ exhibit the variation of pressure difference across the innermost and the outermost layers with inner radius. This is based on Eq. (3.23). This corresponds to $\omega_o = 5$ *cycles* s^{-1}, and $\omega_i = 25$ *cycles* s^{-1}. In the four cases the inner radius varies as (a) $r_i = 0.1$ m, (b) $r_i = 0.3$ m, (c) $r_i = 0.5$ m, (d) $r_i = 0.9$ m.

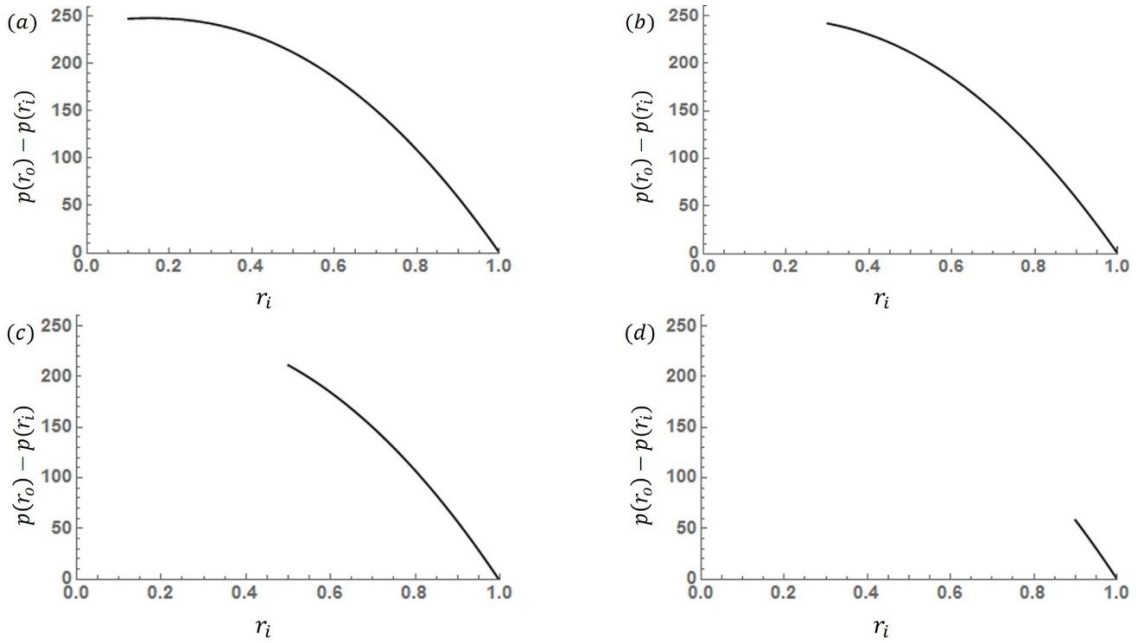

Figure 3.12: The diagrams $(a - d)$ exhibit the variation of pressure difference across the innermost and the outermost layers with inner radius. This is based on Eq. (3.23). This corresponds to $\omega_o = 20\ cycles\ s^{-1}$, and $\omega_i = 25\ cycles\ s^{-1}$. In the four cases the inner radius varies as $(a)\ r_i = 0.1\ m$, $(b)\ r_i = 0.3\ m$, $(c)\ r_i = 0.5\ m$, $(d)\ r_i = 0.9\ m$.

3.4 Conclusions

The most important conclusion with regard to the characteristics of whirlwinds, particularly dust devils, is that a low pressure region is essentially required for the existence of a whirlwind. The radial pressure gradient caused by the variation of temperature creates it. Even when there are no radial temperature gradients, once a region with low pressure is created, it will help the whirlwind survive. Hence, it is never a uniformly distributed high/low pressure rotating mass. The presence of low pressure region inside the whirlwind may be termed as the fundamental characteristic.

Moreover, a whirlwind scales up some height into the sky because there is a favourable pressure gradient in the vertical direction and its absence will let the whirlwind lose its growth and lead to its disappearance. The innermost layer reaches the highest point. It is further concluded that the whirlwind can scale a good height only when the annulus thus formed is thick.

It is further concluded that angular velocity will be uniformly zero if the innermost radius tends to zero. This means there is no whirlwind. This endorses the fundamental characteristic that there must be a zone of low pressure inside the whirlwind with no angular velocity.

The axial velocity has two parts. One of them is due to the inner region of low pressure of the whirlwind. This plays a vital role in the whirlwind dynamics as predicted by the model and it characterises all the phenomena similar to whirlwinds.

Moreover, larger the radial pressure difference across the outermost and innermost layers, thicker will be the whirlwind. Thus, if the radial pressure difference between the outermost and innermost layers is larger, the whirlwind is thicker and consequently, it will last longer.

While discussing the model for variable azimuthal velocity, it was inferred that it is the angular velocity, not the azimuthal velocity, which determines whether a whirlwind will be created or not. Thus, a fundamental parameter for such a fluid motion is the angular velocity and not the azimuthal velocity.

****